Chapter 4

Effect of particle size and europium doping on the emission characteristics of the Sr_2CeO_4 phosphor

4.1 Introduction

Doping of trivalent rare earths into the host can help and modify the emission characteristics of any phosphor. Doping forms an integral part of any material to be synthesized or the core area, be it semiconductors used in display or insulators like phosphor for the display industry **[1, 2]**. Judicious use of the dopants enhances and sometimes changes the emission characteristics of the phosphor. Rare earth based research has been the backbone of the display industry and still the $4f^n$ levels play significant role in enhancing and improving the industry with their charming and fascinating spectroscopic transitions. The rare earth studied for the present case was europium as it gives a lot of information about the host along with other useful information like environment of the host. This rare earth element is the most studied and forms an integral part of many display devices, its transitions are very simple and give valuable information on the host environment. This rare earth element can be doped in two forms viz divalent and trivalent, it requires inert or reducing atmosphere to get into the divalent state. The europium in divalent state has transitions from the $4f^6\ 5d^1$ to lower state whereas for the trivalent state it is generally from the $^5D_0$, $^5D_1$ to the ground state at ^7F_J (where J = 0, 1, 2, 3, 4). Our interest in this work was to monitor and study trivalent Europium, and to see what information it provides about the host in which it has been incorporated. The line emission makes it more appealing to study this rare earth. Till date there are only few reports which have mentioned the doping of tri and tetravalent rare earth ions into the host (Sr_2CeO_4), the efficient mechanism of the emission among them is studied. But there are still no reports of doping by sol-gel synthesis into the host, efficient energy transfer between the host and the guest and their interpretation are still few. To explore this possibility, we have tried to study the energy transfer. One of the first reports on the doping of Sr_2CeO_4 was by Hinatsu et al **[3]**, they studied the EPR of Pr^{4+} in the host and found large tetragonal distortion from octahedral symmetry at Pr^{4+} site. For this chapter we will limit our study only to the Europium doping in trivalent form. The europium doping has been tried previously in the same host **[4-8]** but there are no reports on the doping using sol-gel technique. The main aim is to compare the luminescence characteristics of doped Sr_2CeO_4 by both the sol-gel and the solid state reaction. Though the energy transfer mechanism should

be same for both, there are chances of europium occupying the symmetric or the nonsymmetric sites and thus the emission properties may differ due to the change in the crystal size of the host matrix.

Luminescence of europium in the host has been well studied for its applications in lightening and display phosphor along with laser system [**1, 2, 9-19**] and also as a structural probe for knowing the local environment around the dopant [**9, 20-25**]. Though the f orbital is strongly shielded from the outside ligands, the positions of the spectral lines vary only slightly with the environment, however, their intensities are strongly dependent on the host in which the rare earth is embedded [**26-28**]. The energy levels of the $[Xe]4f^n5d^0$ and $[Xe]4f^{n-1}5d^1$ electron configurations of the lanthanide ions possess two important properties:

(1) The electrons are shielded from the crystalline environment by the outer filled $5s^2$ and $5p^6$ orbitals. As a result the $4f^n$ level energies are determined by interactions within the lanthanide ion.

(2) Chemically the 5d electron possesses similar properties for each lanthanide ion i.e. though the 5d electron has a very strong interaction with the crystal field, the interaction is almost same for each lanthanide [**29**].

To use europium as a tool to know about the environment of the host and the surrounding, doping into the host Sr_2CeO_4 phosphor, we have tried to make use of the same and study that if there is any difference between the transitions by both the synthesis technique. The size plays an important role in the establishing the surrounding of the host and as new sites or the symmetry of the europium defining the radiative transitions and thus the emission characteristics of the compound.

The white light emission can be generated primarily by two ways:

(1) mixing three monochromatic sources (red, green, and blue) and

(2) using phosphors to convert UV or blue light into a combination of red, green and blue or yellow and blue [**30**].

In particular, single phosphors that can emit blue, green, and red are drawing attention as potential white light sources since they offer higher luminous efficiencies and lower manufacturing costs than the systems that require multiple phosphors to achieve the same blend of colors. [**31**].

White light emission from a single host lattice is a hot topic today. The quality of the white light depends on many factors namely, the correct blue-to-yellow intensity ratio, density, particle size of phosphor and the coating quality [**32, 33**] The phosphor research impetus has increased for making better red, green and blue phosphor. The phosphor devices should have high resolution, high packing density (also require low binder content) and higher brightness for better performance, this can be achieved only when the size of the particle is very small [**13, 15, 34, 35**]. The sol-gel method offers many advantages over the conventional solid state and others techniques as we have reported in our paper [**36**]. However the purity of the host matrix and the homogeneity of the activators are very important criteria for making efficient phosphors. The surface area of the powders produced from the sol-gel is very high leading to lowering of processing temperature and time. The sol-gel process minimizes the cross contamination of the phosphors thus made and with smaller size the probability of the electron and hole capture to the impurity increases and the electron-hole localization enhances the recombination rates [**34**].

As the luminous intensity also plays an important role, we also synthesized the compound, Sr_2CeO_4 [**36**]. Sr_2CeO_4 is a phosphor with 100% active center concentration, thus all CeO_6 octahedra may be considered as fluorescent centers and quantum efficiency is very high [**5**]. Sr_2CeO_4 might also act as a sensitizer to transfer the absorbed energy to the dopants (activator), because of the possibility of energy transfer from Sr_2CeO_4 to the dopant ions. Various concentrations of rare earth were doped in the compound. Green and red luminescence was also observed from $Sr_2CeO_4:Eu^{3+}$, and thus the white light emission were observed at an appropriate concentration of europium. Though at present calcium halo phosphate is a well known white luminescence material under UV (254nm) excitation. Phosphors for white light emission or triband phosphor are also available but for them an appropriate mixing of blue ($BAM:Eu^{2+}$), Green ($(Gd,Ce^{3+},Tb^{3+})MgB_5O_{10}$) and Red ($Y_2O_3:Eu^{3+}$) is needed. In this regard $Sr_2CeO_4:Eu^{3+}$ can also act as an efficient white light emitter considering its property of emitting sharp emission in the visible region from a single host lattice.

However, only a few papers have been published about the doping of rare earth ions in Sr_2CeO_4. As per our knowledge till this date sol-gel synthesized trivalent

rare earth doped Sr_2CeO_4 has not been reported. This chapter mainly deals with the preparation and characterization of Sr_2CeO_4 doped with various concentrations of europium using sol-gel as well as by Solid state reaction technique. The mechanism and the energy transfer along with the different light emissions, (blue to green yellow to white to red) at different concentrations of Europium, from the single host lattice has been explained in details.

4.2 Experimental

The synthesis technique has been elaborated in chapter three of this thesis by both the sol-gel and the solid state reaction. The doping of the europium into the phosphor was done at the initial stage of the reaction using the Eu_2O_3 (99.9%) purchased from S.D. Fine chemicals. For some of the synthesis in the sol-gel case the Eu_2O_3 was first dissolved with concentrated HNO_3 (36%w/v) from Merck, Mumbai, heated and then washed several times with double distilled water. The powders were weighed according to the nominal composition of $Sr_{1-x/2}(NO_3)_2+Ce(NO_3)_3.9H_2O+xEu(NO_3)_3$ (where x = 0.5%, 1%, 1.5%, 2% and 4%). For the solid state reaction $SrCO_3$, CeO_2 and Eu_2O_3 (0.5%) were also made for comparison with sol-gel at two different sites.

The reaction mechanism can be explained by the simple equation as:

$$\mathbf{2Sr_{1-x/2}(NO_3)_2+Ce(NO_3)_3.9H_2O+xEu(NO_3)_3 \rightarrow Sr_{2-x}CeO_4:xEu}$$

4.2.1 Characterization

4.2.1(a) X-ray Diffraction studies

Phase identification of the powders was carried out by the X-ray powder diffraction using RIGAKU D'MAX III Diffractometer having Cu Kα radiation (λ= 0.154nm). The scan range was kept from 5 degrees to 80 degrees at the scan speed of 0.05 degree per second.

4.2.1(b) Scanning Electron microscope (SEM)

The Scanning Electron Micrograph images (SEM) of the samples were taken using JEOL make JSM-5610 LV for studying the morphology of the compound, details in chapter two of the thesis.

4.2.1(c) Photoluminescence measurements

The photoluminescence (Emission and Excitation spectra) were recorded at room temperature using spectrofluorophotometer RF-5301 PC of SHIMADZU make, details in chapter two of this thesis. The source used in this is a xenon lamp. The slit width for the emission and excitation was kept at 1.5nm for all the measurements. A filter was used to remove the second order peak of the excitation light in the PL measurements. The sensitivity of the instrument was set as high unless stated otherwise.

4.2.1(d) Commission Internationale de l'Eclairage (CIE) coordinates

For the present study, the *Equidistant-Wavelength method* has been used to determine the coordinates on the colorimetric chromaticity diagram. The CIE coordinates for the samples have been calculated for CIE 1931, CIE 1960 and CIE 1976, details have been given in chapter two.

4.3 Result and Discussion

4.3.1 X-ray diffraction studies

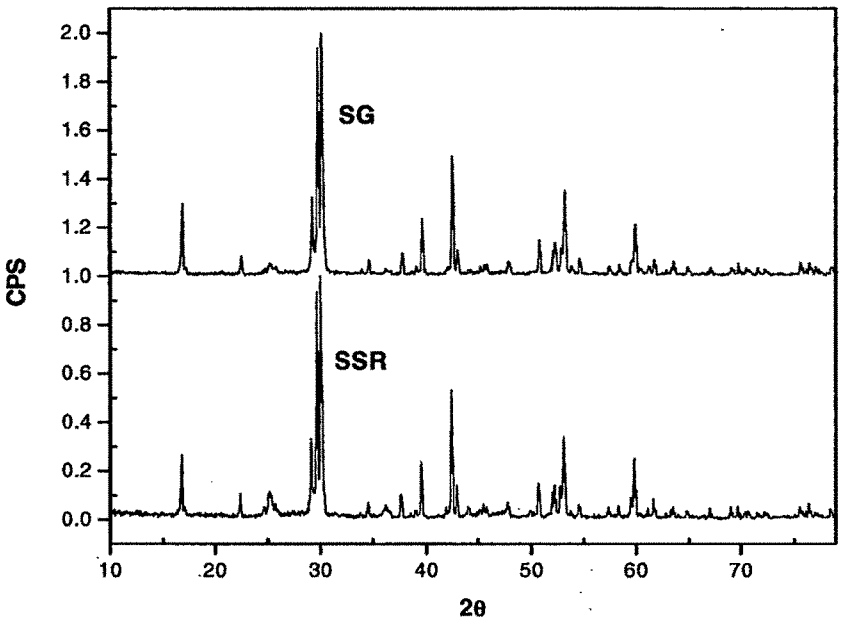

Figure-1 The X-ray diffraction pattern of the europium doped Sr_2CeO_4 syntheiszed with sol-gel and solid state reaction technique.

The figure-1 shows the powder X-ray diffraction pattern of the synthesized phosphor sample. The result shows that the phase of the material is almost pure with traces of $SrCeO_3$ present in it a bit. The average crystallite size was calculated using the Scherrer formula

$$d = \frac{k\lambda}{\beta \cos \theta_B},$$

Where k = Constant (0.9), λ = Wavelength of the X-ray (0.154nm in the present case), β = full width at half-maxima (FWHM), θ = Bragg angle of the XRD peak. The crystallinity of the compound as revealed by the XRD pattern, increased on raising the calcining temperature. This was also observed by Shikao Shi et al. [8]. From the analysis of the XRD pattern, it was understood that the introduction of activator Eu^{3+} did not influence the crystal structure of the phosphor matrix. The calculated average crystal size of the sample calculated by measuring the full

width half maxima was found to be of about 55nm for europium 1mol% doped sample.

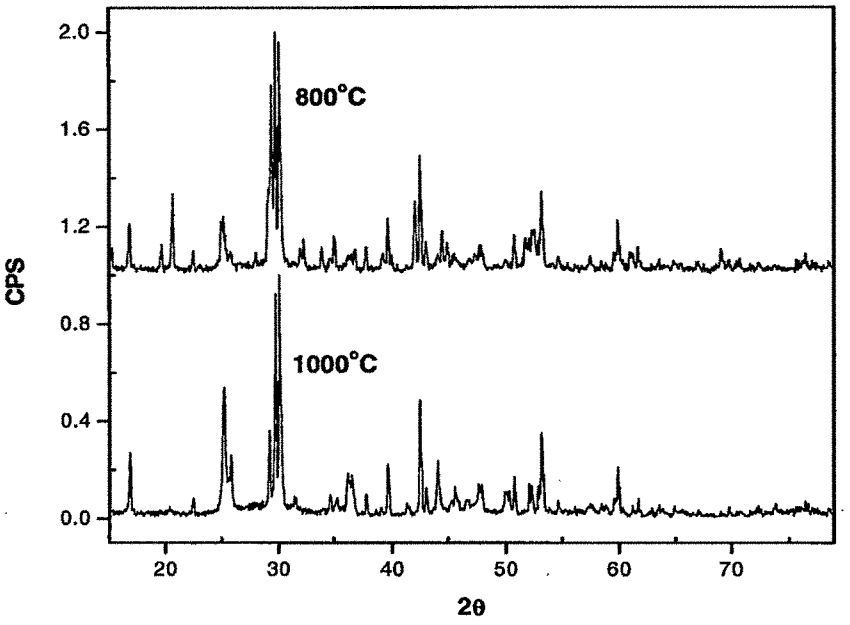

Figure-2 The X-ray diffraction pattern of the europium doped Sr_2CeO_4 syntheiszed with sol-gel technique (heated at different temperatures).

Figure-2 is the sol-gel synthesized Sr_2CeO_4 sample heated at different temperatures of 800°C and 1000°C. it is observed form both the curves that the pure Sr_2CeO_4 has not formed at these temperatures, but there are many peaks belonging to the $SrCeO_3$, CeO_2, SrO which do not appear at 1200°C as seen from figure-1. This concludes that if the pure phase has to be achieved then the sample has to be heated treated at1200°C.

4.3.2 Scanning Electron Microscopy

The micrographs of the sample are prepared from the sol-gel route (doped and undoped) have been shown below (figure-3).

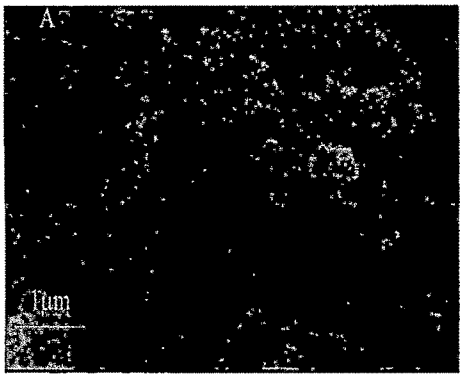

A. Sol-Gel synthesized doped Eu(0.5mol%)

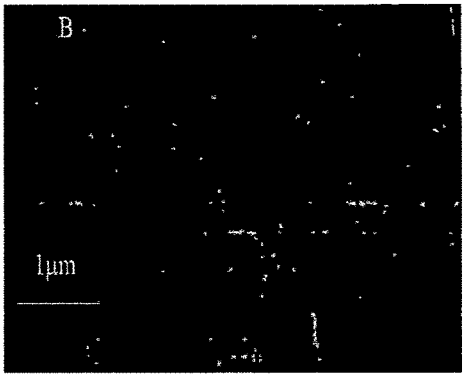

B. Sol-Gel synthesized doped Eu(1.0mol%)

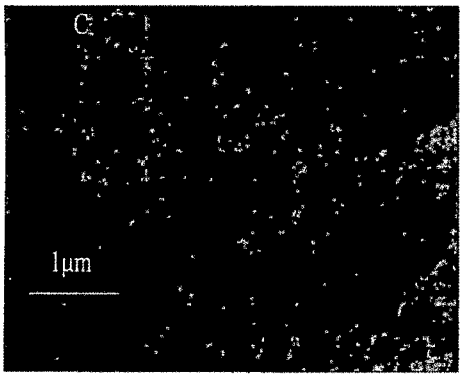

C. Sol-Gel synthesized doped Eu(2.0mol%)

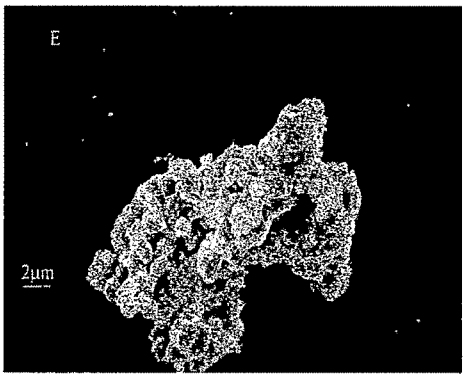

E. Sol-Gel synthesized undoped

Figure-3 Micrographs of the Europium doped Sr_2CeO_4 and one plain shown for comparison.

The SEM studies from different synthesis routes have been elaborated and discussed in the previous chapter. The above micrographs are the of the sample prepared with sol-gel at different europium concentrations. From the SEM micrographs one can see that the morphology of the samples prepared by the sol-gel, it appears that the shape of the sol-gel prepared are spherical and they appear to be less agglomerated. They also show narrow size distribution which means that all the particles are of almost same size. The spherical morphology has a positive effect on the optical property, as the scattering of the light is less and hence it directly influences the luminescence intensity and will be discussed in the photoluminescence section.

4.3.3 Photoluminescence Spectra

4.3.3(a) Luminescence of Europium doped Sr_2CeO_4

4.3.3.1 (a) Emission spectra of Europium doped Sr_2CeO_4

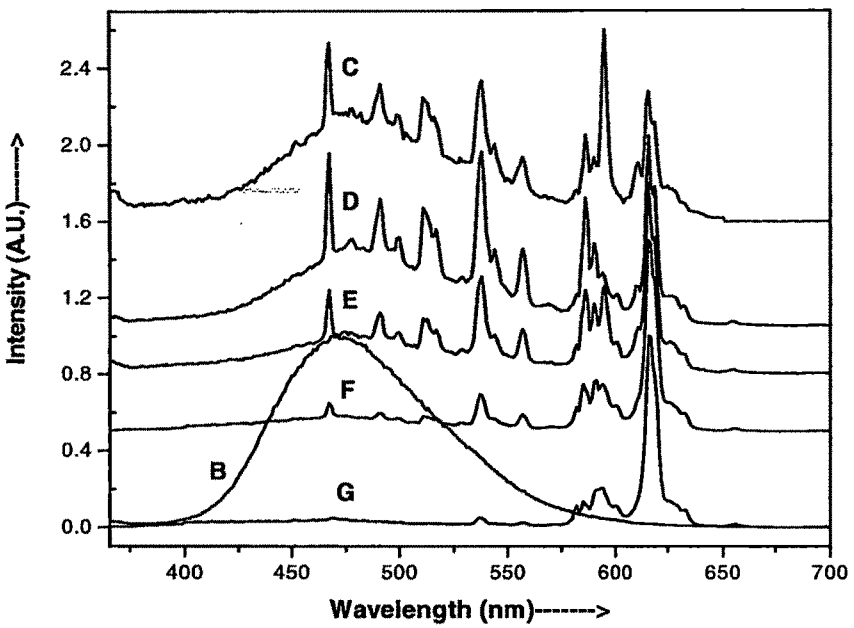

Figure-4 The photoluminescence emission spectra of the europium doped Sr_2CeO_4 Sol-Gel synthesized sample at different europium concentration with 254nm of wavelength.

Trivalent rare earth dopant can be an efficient mode for observing any energy transfer in the host lattice i.e. from Sr_2CeO_4 when europium was doped. The emission spectra of the Sr_2CeO_4 sample doped with europium at different mole percentage was recorded with the excitation kept at 254nm at room temperature and has been shown in the figure-4.

Sr. No.	Sample Name	Percentage of Europium
1	Sr_2CeO_4 Curve B	0.0
2	Sr_2CeO_4 Curve C	0.5
3	Sr_2CeO_4 Curve D	1.0
4	Sr_2CeO_4 Curve E	1.5
5	Sr_2CeO_4 Curve F	2.0
6	Sr_2CeO_4 Curve G	4.0

Table-1: Mole percentage of Europium and the curves marked in figure-4.

The table-1 depicts the mole percentage of Europium doped to the phosphor Sr_2CeO_4. The emission spectra for Sr_2CeO_4 (curve-B) shows a broad band due to $f \rightarrow t_1g$ of Ce^{4+} around 469 nm. This emission spectrum is assigned to the Ce^{4+}-O^{2-} charge transfer transitions [37]. The emission spectra for europium doped show transitions starting from 467nm to 656nm. The interesting feature of these spectra is the appearance of europium transition from $^5D_2 \rightarrow {}^7F_0$ (467nm) which is very rare, since the general oxide host have higher photon energy and thus a nonradiative loss from a higher 5D state occurs due to multiphonon relaxation [6]. There are few transitions which are magnetic dipole (MD) like $^5D_0 \rightarrow {}^7F_1$, $^5D_1 \rightarrow {}^7F_0$ and $^5D_2 \rightarrow {}^7F_1$ rest all of the transitions that appear are the electric dipole (ED) due to the intra-$4f^6$ transitions.

Wavelength (nm)	Transitions	Energy (eV)	Energy (cm^{-1})
467	$^5D_2 \rightarrow {}^7F_0$	2.657	21413
478	$^5D_2 \rightarrow {}^7F_1$	2.596	20920
483	$^5D_2 \rightarrow {}^7F_2$	2.567	20703
491	$^5D_2 \rightarrow {}^7F_2$	2.528	20366
500	$^5D_2 \rightarrow {}^7F_2$	2.482	20000
511	$^5D_2 \rightarrow {}^7F_3$	2.429	19569
515	$^5D_2 \rightarrow {}^7F_3$	2.410	19417
529	$^5D_1 \rightarrow {}^7F_0$	2.350	18939
538	$^5D_1 \rightarrow {}^7F_1$	2.307	18587
544	$^5D_1 \rightarrow {}^7F_1$	2.281	18382
557	$^5D_1 \rightarrow {}^7F_2$	2.228	17953
569	$^5D_1 \rightarrow {}^7F_3$	2.179	17574
577	$^5D_1 \rightarrow {}^7F_0$	2.148	17331
580	$^5D_0 \rightarrow {}^7F_0$	2.137	17241
586	$^5D_0 \rightarrow {}^7F_1$	2.118	17064
590	$^5D_0 \rightarrow {}^7F_1$	2.103	16949
595	$^5D_0 \rightarrow {}^7F_1$	2.086	16806
601	$^5D_0 \rightarrow {}^7F_2$	2.063	16638
611	$^5D_0 \rightarrow {}^7F_2$	2.031	16366
616	$^5D_0 \rightarrow {}^7F_2$	2.015	16253
619	$^5D_0 \rightarrow {}^7F_2$	2.003	16155
627	$^5D_0 \rightarrow {}^7F_3$	1.977	15948
632	$^5D_0 \rightarrow {}^7F_3$	1.961	15822

Table-2 Energy levels of Eu^{3+} doped in Sr_2CeO_4 observed in emission spectra at room temperature.

The table-2 shows the energy of the all the transitions, the intensity of the transition at $^5D_0 \rightarrow {}^7F_0$ is very less as this transition is forbidden by both the ED and MD selection rules. As the doping percentage was increased from 0.5mol% to 4.0mol% the transition appearing at lower wavelength (>580nm) get diminished and the only transitions observed are $^5D_0 \rightarrow {}^7F_J$ (where J = 0, 1, 2, 3). It seems that at low europium concentration the energy transfer is incomplete and it is highly probable that the CT band of Eu^{3+} in Sr_2CeO_4 lies in higher energy region and the energy migration takes place at higher concentrations. The emission spectra of the higher concentration of europium in Sr_2CeO_4, under 254nm excitation, depict only the Eu^{3+} transitions/lines and the Ce^{4+} emission is totally quenched. From this result, we may conclude that at the higher concentration of europium (<4%) the energy is totally transferred from Ce^{4+}-O^{2-} CT emission band to Eu^{3+}. Similar results were also observed by Sanker et al. [4].

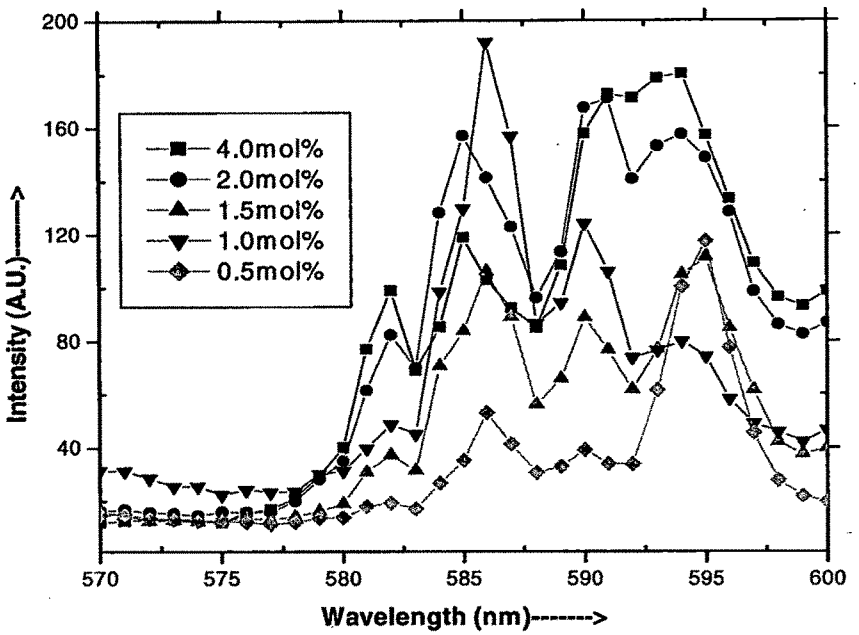

Figure-5 The Photoluminescence emission spectra (578-594nm) of the sol-gel synthesized Sr_2CeO_4 at different europium concentrations excited with 254nm wavelength.

Figure-5 is the extended emission spectra for different concentration of europium doping from 578-594nm. There is however some emission from $^5D_2$ level also at low concentrations of Eu^{3+} ions, $^5D_2 \rightarrow {}^7F_0$ as seen in emission spectra (Figure-4). Thus in the emission process, a competition takes place between $^5D_2$ and $^5D_0$ emission which is dependent on Eu^{3+} ion concentration. The reason behind the emission from different levels is that the PL spectra was measured at room temperature hence there is stark splitting of the components which results in various emission transitions. This effect can be rectified by measuring the PL spectrum at lower temperature. The $^5D_0 \rightarrow {}^7F_0$ is a $0 \rightarrow 0$ transition and no crystalline electric filed (Crystal Field) will be able to split the level i.e. no stark components will be observed. This transition therefore, can ensure the single occupancy of Eu^{3+} ions in the crystalline sites of the host. If there are more than one splitting seen for $^5D_0 \rightarrow {}^7F_0$ transition then one can conclude that Eu^{3+} ions occupy two or more sites. It can therefore be used for monitoring the homogeneity of the material also. In case of 1mol% doped europium the homogeneity of the phosphor can be observed. It is also observed from the peaks

around 580-590nm that as the concentration increases beyond 1mol% europium, the peak at 587nm shifted towards lower wavelength i.e., around 585nm and also a peak at 582nm starts appearing with higher concentration showing that the europium ions occupy two different sites. The $^5D_0 \rightarrow {}^7F_0$ transition of Eu^{3+} is a parity forbidden transition; hence it is commonly utilized to deduce the number of luminescent sites in the phosphor material. The dual occupancy of the luminescent sites in the nanocrystals was also observed by Wei et al [22].

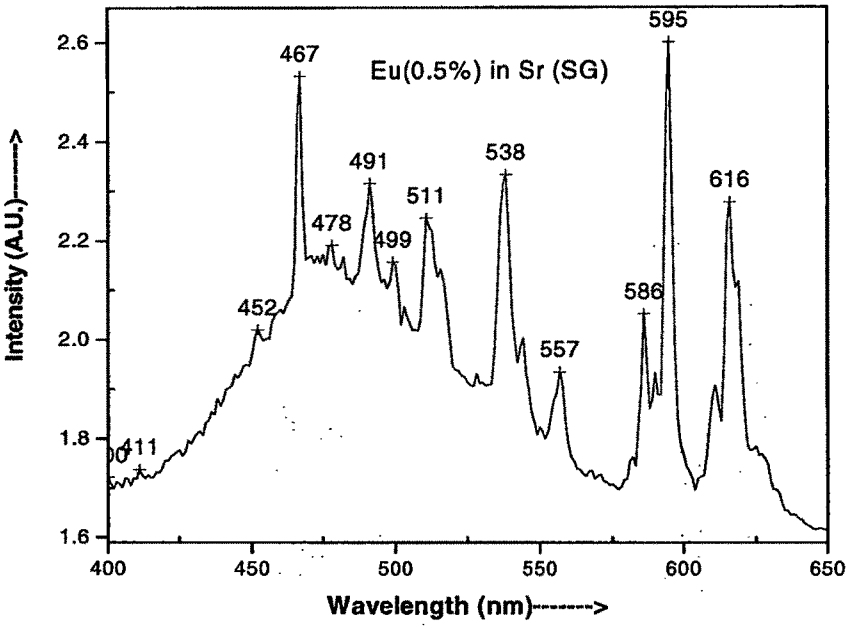

Figure-6 The Photoluminescence emission spectra of the sol-gel synthesized Sr_2CeO_4 with europium (0.5mol%) doping excited with 254nm wavelength.

The emission spectra of the europium (0.5mol%) doped in Sr site by sol-gel has been shown in figure-6. The peak at 595nm is highest in intensity for the $^5D_0 \rightarrow {}^7F_1$ transitions and even higher than that at 467nm ($^5D_2 \rightarrow {}^7F_0$) but as the percentage of europium doping is increased the intensity of this decreases. The stark splitting for the $^5D_0 \rightarrow {}^7F_1$ would be three (2J+1) theoretically and experimentally all the three are observed with the intensity of the 595nm being highest, increasing the concentration decreases it with subsequent increase of the 586nm intensity. This is unique observation for the 0.5mol% doped and not for

all. The stark splitting for $^5D_0 \rightarrow {}^7F_2$ would be five theoretically and four lines are found experimentally.

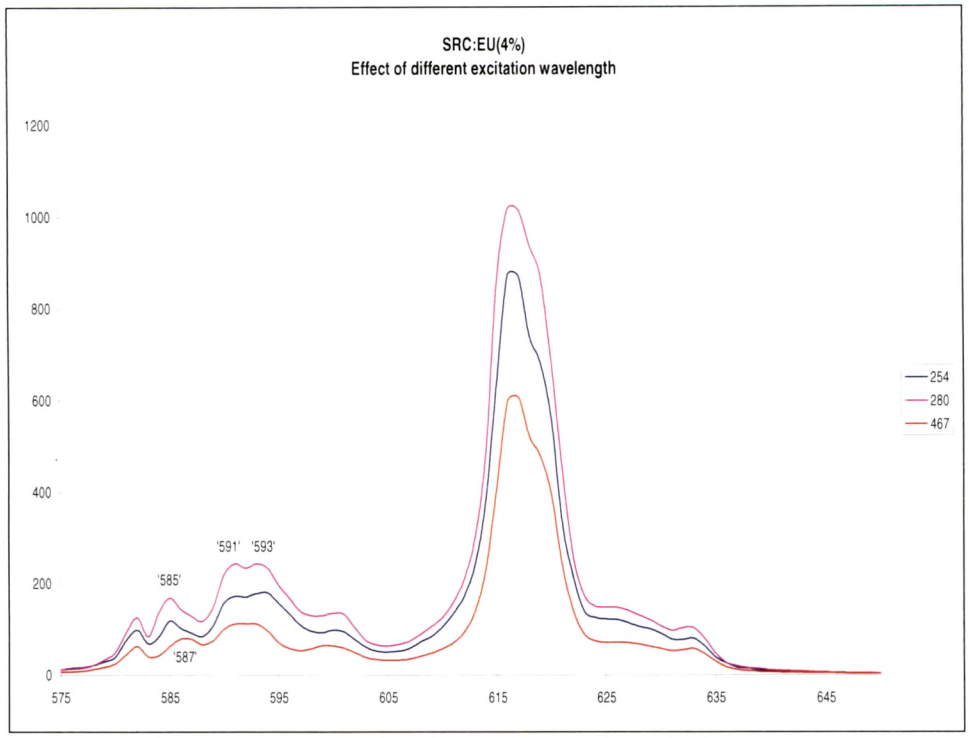

Figure-7 The Photoluminescence emission spectra of the sol-gel synthesized Sr_2CeO_4 with europium (4.0mol%) doping excited with 254nm wavelength.

The emission spectra measured for different excitation wavelengths i.e. 254nm, 280nm and 467nm respectively is shown in the figure-7. It is observed that the emission is highest for the 280nm wavelength and the emission pattern is same for excitation wavelengths except for 467nm. The emission observed from 467nm excitation wavelength shows minor changes than the other two. As the emission coming from 467nm is not governed by charge transfer band hence we can see the small shift of the 585nm peak towards higher wavelength region, the stark splitting of the $^5D_0 \rightarrow {}^7F_1$ transitions is also not clear. These results confirm that the different excitation wavelength can change the composition of different sites spectrum components.

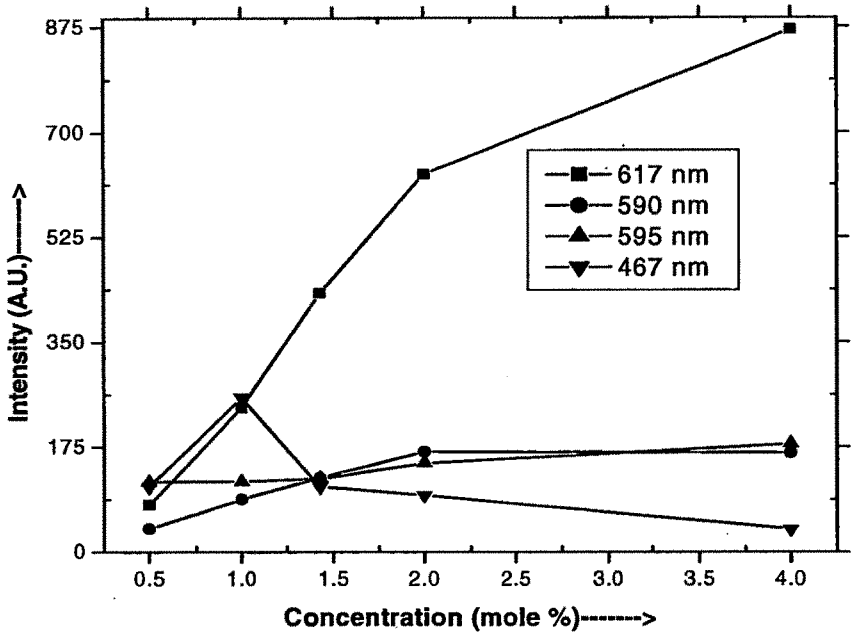

Figure-8 The variation of intensity with different concentrations on various peak wavelengths of the sol-gel synthesized Sr_2CeO_4 with europium doping.

The effect of different concentration on the various emission wavelengths is shown in above figure-8. From this figure it is observed that as the concentration of europium increases from 0.5% to 4mol%, the emission intensity at 616nm goes on increasing showing the dominant transition from $^5D_0 \rightarrow ^7F_2$ level. The transition from $^5D_0 \rightarrow ^7F_1$ level i.e., the intensity of 590nm increases from 0.5mol% to 2mol% by a small fraction and then it saturates onwards. The intensity at the 595nm hardly varies with the concentration. The emission at 467nm reaches its maxima at 1% europium concentration and then decreases with increase in the concentration. This emission corresponds to the $^5D_2 \rightarrow ^7F_0$ transition of Eu^{3+}. The transition around 600-620nm is due to the electric dipole (ED) transition of $^5D_0 \rightarrow ^7F_2$ which is induced by the lack of inversion symmetry at the Eu^{3+} sites and is much stronger than the $^7F_1$ transition.

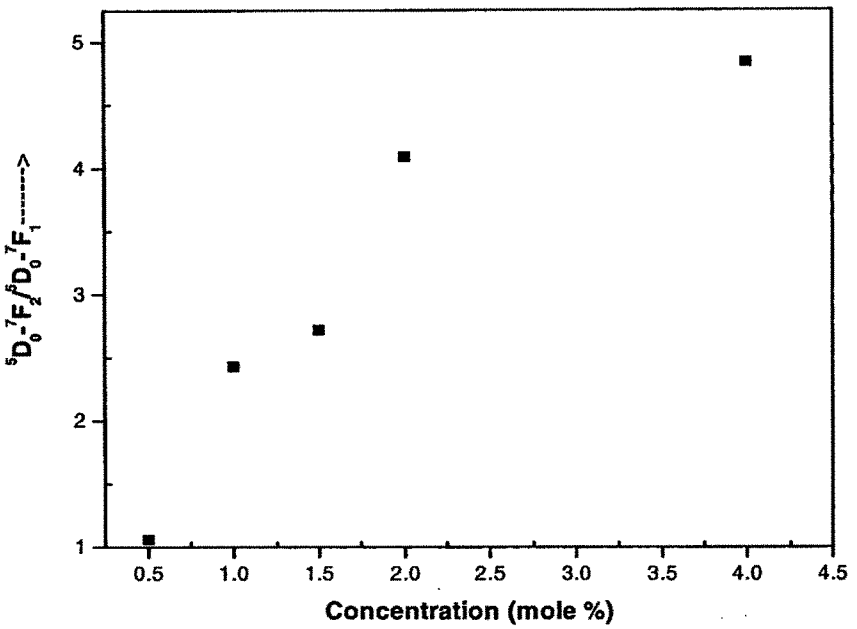

Figure-9 The relative intensity ratio of $^5D_0 \rightarrow {}^7F_2$ to $^5D_0 \rightarrow {}^7F_1$ transitions at different concentrations of europium.

It is well known; the $^5D_0 \rightarrow {}^7F_2/{}^5D_0 \rightarrow {}^7F_1$ intensity ratio is a good measure of the site symmetry of the rare earth ions/doped material, it has been shown in figure-9. This is because the hypersensitive transition $^5D_0 \rightarrow {}^7F_2$ tends to be much more intense in an inversion symmetry site, while the magnetic dipole transition $^5D_0 \rightarrow {}^7F_1$ is constant, regardless of the environment [2]. The larger $^5D_0 \rightarrow {}^7F_2/{}^5D_0 \rightarrow {}^7F_1$ intensity ratio indicates that the point symmetry of Eu^{3+} site is closer to an inversion center. It is conceivable that there are a large number of different local atomic structures in the boundary region in which the Eu^{3+} ions will present the broad feature in the spectroscopy. And due to the disordered boundary component, the Eu^{3+} site in the boundary layer can show symmetry closer to an inversion center than the interior crystallographic site that is less inversion symmetric [38]. The intensity of the hypersensitive transition $^5D_0 \rightarrow {}^7F_2$ indicate that Eu^{3+} ions prefers to occupy a low symmetry site. Such an Eu^{3+} could be accommodated at the surface of the nanocrystal. This is because, in a real nanocrystalline solid, the atoms in the grain boundary region are likely to be displaced from their lattice positions to new, non-lattice equilibrium positions. The distribution of these nonlattice atoms in the boundary region may be

disordered, and/or short-range ordered [38]. It is conceivable that there are a large number of different local atomic structures in the boundary region in which the Eu^{3+} ions will present the broad feature in the spectroscopy. And due to the disordered boundary component, the Eu^{3+} site in the boundary layer can show a symmetry closer to an inversion center than the interior crystallographic site that is less inversion symmetric. Overall resolution of individual peaks is very good for 1mol% Eu^{3+} as compared to 4mol% sample. Dual occupancy of Eu^{3+} ions is equal for 4mol% sample while it is quite uneven for 1mol% sample.

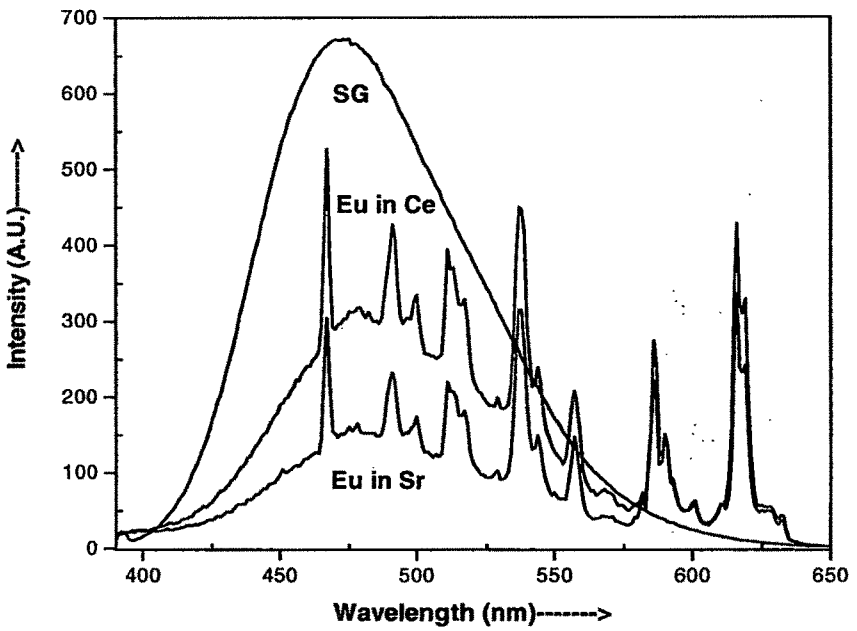

The role of net effective charge of the crystal in deciding the luminescence efficiency of the dopant ion in the lattice under CT transition is one of an important parameter, if the charge of the lattice is negative then the efficiency will increase in the case of the lanthanide ions and vice versa. The ionic radii of the Sr^{2+}, Ce^{4+} and Eu^{3+} are 118pm, 87pm and 95pm respectively, these are also tabulated in table-3 [39], when the Europium is doped in the compound it may prefer to occupy the Sr^{2+} crystallographic site rather than the Ce^{4+} site since their

ionic radii matches (Eu^{3+} and Sr^{2+}). An attempt is made to study the influence of the net charge on the luminescence efficiency. The comparative study by doping of Eu^{3+} at different sites was done (Eu^{3+} replacing Sr^{2+} and Eu^{3+} replacing Ce^{4+}). Both the samples were prepared by solid state reaction, doped with 0.5mol% of Europium (0.5mol%) at Cerium and Strontium sites respectively. The photoluminescence emissions displayed by both the phosphor are presented in figure-10 (Sol-gel prepared Sr_2CeO_4 sample is shown for comparison). On doping Eu^{3+} on Ce^{4+} sites the net charge becomes negative and also the charge transfer bands of the Ce^{4+} and Eu^{3+} are found to resemble each other in character [4] whereas on doping Eu^{3+} in Sr^{2+} sites the net charge of the crystal lattice becomes positive. The interesting and an important observation in this is that the intensity of the $^5D_0 \rightarrow {}^7F_2$ transitions is greater than all the transition of the Europium observed when europium was doped in the Strontium sites whereas for the other it was the same as in the case of sol-gel. Apart from these, photoluminescence emission from both the materials displays almost the same result.

Ion	Charge	Coordination	Ionic Radius
Ce^{4+}	4	VI	0.87
Eu^{3+}	3	VI	0.947
		VII	1.01
Sr^{2+}	2	VI	1.18
		VII	1.21

Table-3 The ionic radii along with their coordination.

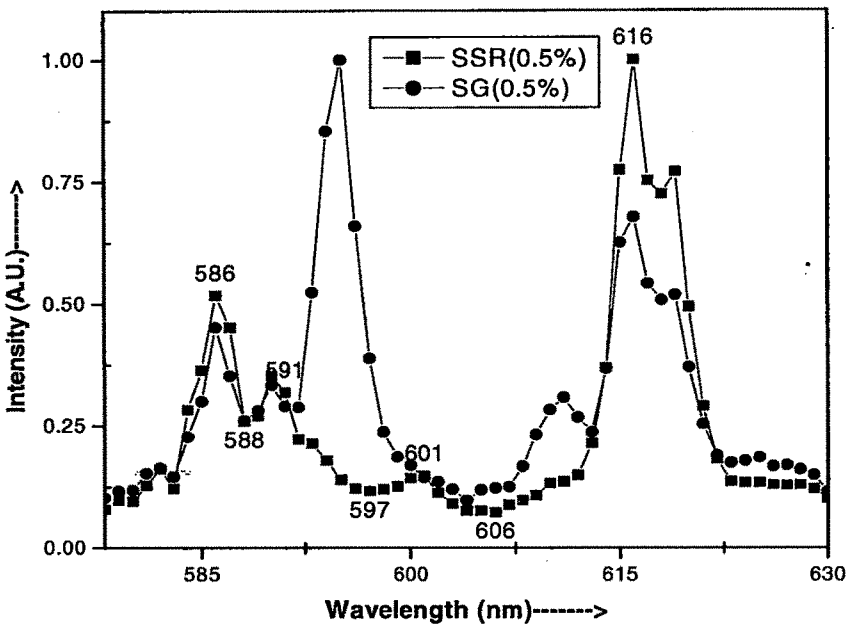

Figure-11 Comparison of Sol-Gel and solid state synthesized Sr_2CeO_4 with europium (0.5mol%) doping.

Comparison between sol-gel and the solid state reaction sample for europium 0.5mole % has been shown in figure-11. There is a remarkable difference in the emission spectra of the sol-gel and solid state reaction technique, the spectra is almost similar at all the wavelengths except at the 580-630nm. The most important difference is the generation of the high intensity 595nm peak and with small hump at 611nm for the sol-gel sample which is not seen in the solid state reaction sample. These are due to splitting of $^5D_0 \rightarrow {}^7F_1$ and $^5D_0 \rightarrow {}^7F_2$ transition levels which are not observed in the solid state reaction specimen. This shows that the crystal field splits the levels ($^7F_1$ and $^7F_2$).

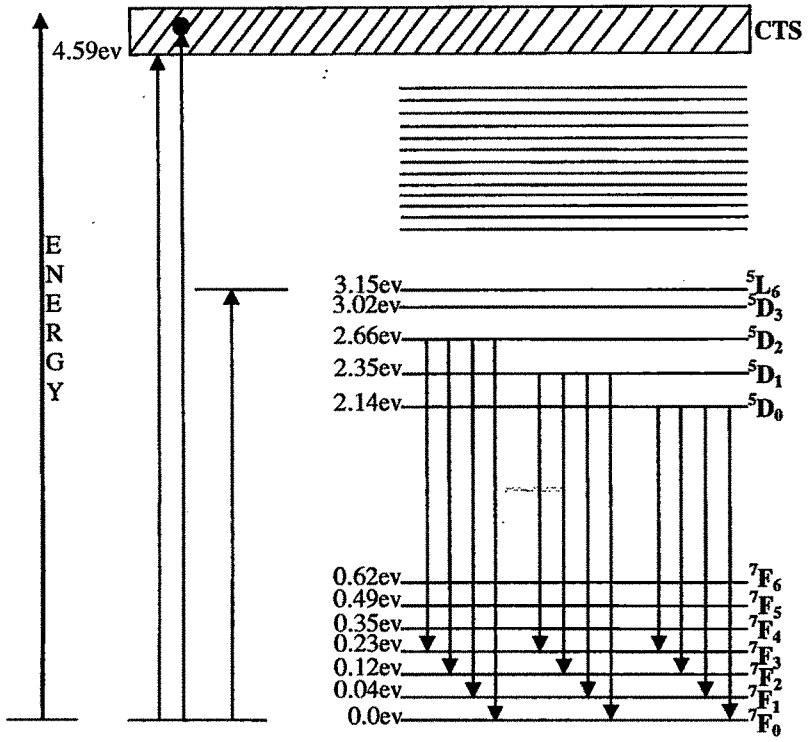

Figure-12 The transitions of Europium doped in Sr_2CeO_4 phosphor.

The well known Eu^{3+} transitions as seen in the Sr_2CeO_4 doped nanocrystals, have been shown in figure-12. Observed excitation and emission transitions are represented in the figure. In summary, we say that the 254nm photons are absorbed by the (t_{1g}-f) CT band of Sr_2CeO_4 transition and nonradiatively transferred to the charge transfer state of Eu^{3+} where upon the nonradiative transitions occur until the electron reside in the different energy level in the 4f shell and the radiative recombination then occurs to ^7F_J levels, with $^5D_0 \rightarrow {}^7F_2$ being the most intense one **[35]**.

4.3.3.1 (b) Excitation spectra of Europium doped Sr_2CeO_4

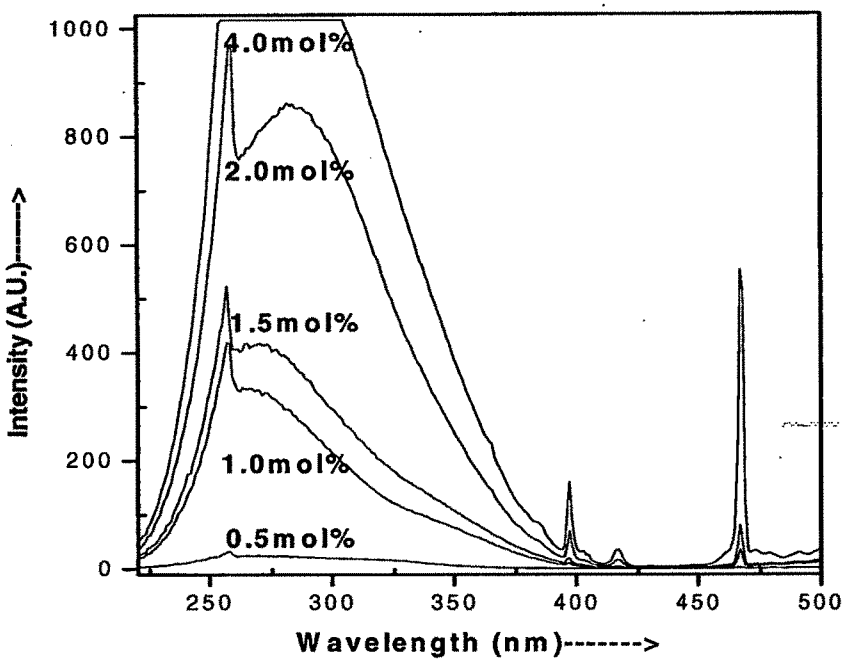
1000
800
600
400
200
0
Intensity (A.U.)------>
4.0mol%
2.0mol%
1.5mol%
1.0mol%
0.5mol%
250
300
350
400
450
500
Wavelength (nm)------->

Figure-13 The Photoluminescence excitation spectra of the Europium doped Sr_2CeO_4 synthesized by sol-gel technique.

The figure-13 shows the excitation spectra of $Sr_2CeO_4:Eu^{3+}$ (when monitored with 617nm wavelength) measured at room temperature. It was found that at low concentration of Eu^{3+}(less than 2mol%) only the charge transfer excitation band at 254nm of Ce^{4+} is observed, but as the concentration of the Eu^{3+} increases (≥2mol%) the excitation band shows the characteristic lines at 397, 417 and 467nm, along with the charge transfer band of Ce^{4+}, due to the transitions $^7F_{0,1} \rightarrow {}^5L_6$ and $^7F_0 \rightarrow {}^5D_2$ respectively of Eu^{3+}. The excitation spectrum shows presence of a strong peak at 467 nm at high concentration of europium (≥2mol%). This shows that the absorption of energy takes place in $^5D_2$ level ($^7F_0 \rightarrow {}^5D_2$). However, there is a non-radiative transition from $^5D_2 \rightarrow {}^5D_0$ from where emission starts showing up with a high peak intensity for $^5D_0 \rightarrow {}^7F_2$ transition. This is possible at high concentration of Eu^{3+} ions.

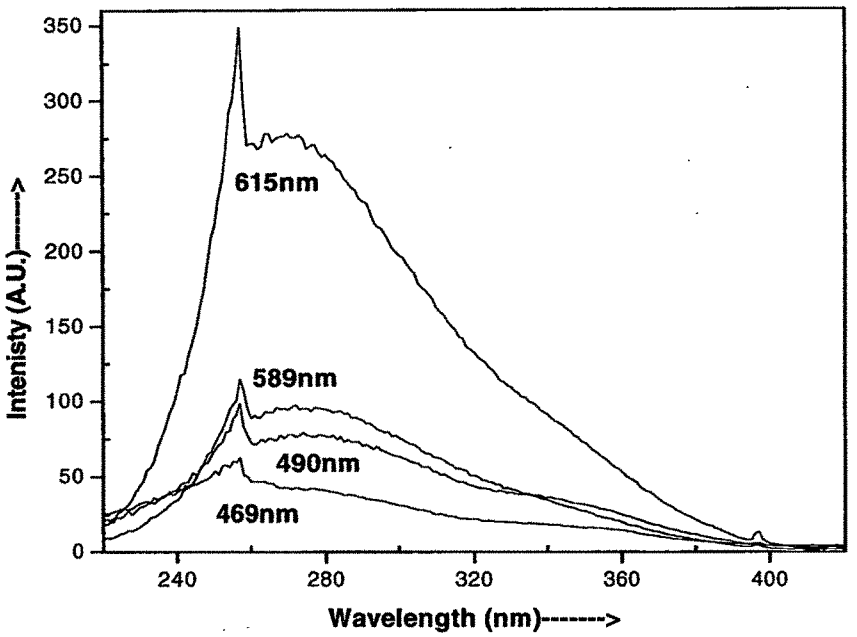

Figure-14 The Photoluminescence excitation spectra for the 4.0mol% europium doped sample monitored at different wavelengths.

The figure-14 is the excitation spectra for the 4.0mol% europium doped sample monitored at different wavelengths. It is observed that changing the monitored wavelength changes the intensity of the excitation spectra. The excitation spectra follow the same pattern for the entire emission wavelength. In our case, from this study we can say that occupancy of Eu^{3+} ions at two different sites are present but the existence of different local environment is totally ruled out. At higher concentration the stark splitting becomes negligible and this can be seen from the emission peak of 4mol% europium doped sample, where the splitting of the $^5D_0 \rightarrow {}^7F_2$ merged into single peak.

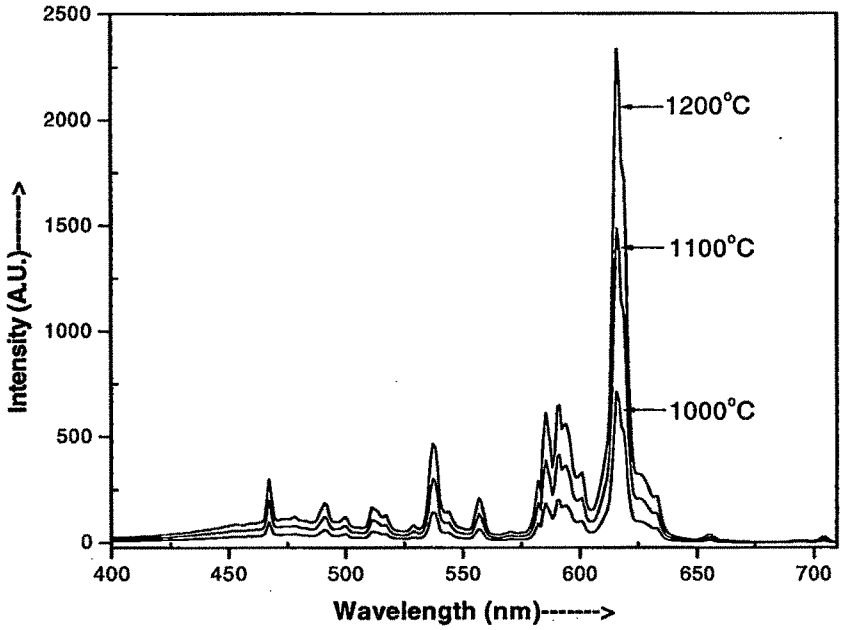

Figure-15 The effect of calcination temperature on the sol-gel synthesized phosphor Sr_2CeO_4 doped Europium(2.0mol%).

It is a well known fact that the crystallanity of the material increases with increase in the calcination temperature. Hence to study the effect of calcination temperature on the sol-gel synthesized phosphor ($Sr_2CeO_4:Eu^{3+}$(2.0mol%)), the phosphor was fired at various temperatures 1000°C, 1100°C and 1200°C for 2hrs respectively. From the figure-15, it is clear that the photoluminescence intensity increases with increase in the calcination temperature. No definite inferences regarding the peak shift with respect to different annealing temperature can be drawn.

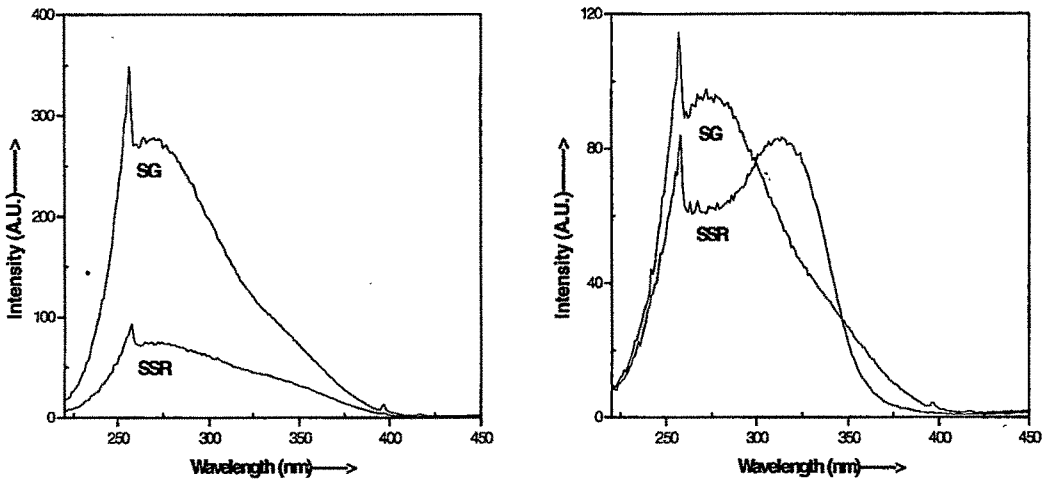

Figure-16 The photoluminescence excitation spectra of the Sol-gel and solid state synthesized samples shown for comparison with wavelength monitored at 615nm(L) and 595nm(R) respectively.

To determine the effect of nano particle size of the phosphor on the emission or excitation, the PL excitation spectra is a basic tool that can be applied to study the effect. In the figure-16, when the excitation spectra of the sol-gel and solid state synthesis phosphor with europium (0.5mol%) doping was compared, the difference in the spectra is clearly observed. The figure towards left represents, the wavelength of the sample monitored at 615nm, whereas the figure towards right is monitored with 595nm. We observe that the intensity of the sol-gel synthesized phosphor is quite high as compared to that of the solid state reaction samples when monitored with 615nm. Whereas, the figure left shows the effect of nano size and the macro size particles. The excitation spectra of the sol-gel synthesized phosphor shows the peak at 254nm and a hump at around 280nm, the excitation spectra of the solid state reaction synthesized samples shows the peak at 254nm but a shift of hump in the red region is observed with peak at around ~320nm, when monitored wavelength was 590nm (the figure towards right). This emission wavelength corresponds to the $^5D_0 \rightarrow {}^7F_0$ transition of the Eu^{3+} ions which are used as the probe to find the homogeneity of the sample. Hence the occurrence of different peaks at the excitation spectra could probably be correlated with the existence of different phases. Also the XRD pattern also shows the existence of some different phases in the XRD pattern of the SSR sample. Hence from these two studies it is clear that the SSR synthesized

phosphors does not give the homogenous phosphor formation. This peak (hump) shift indicates that as the particle size increases, as already elucidated from the X-ray diffraction pattern, from nano to few micro the excitation of the phosphor shows red shift.

4.3.4 CIE coordinates

The value of the CIE coordinates have been calculated by the equidistant wavelength method as described in chapter-2 of this thesis. The values calculated for different concentration sample has been shown in table-4. The values of the without doping Sr_2CeO_4 have been shown for comparison, as the values of the concentration of europium is increased from 0.5mol% to 4.0mol% there is remarkable shift in the CIE coordinates and the appearance of blue colour shifts to bluish green to white, pink and finally towards red. The tuning of the colour by proper doping of the europium is a very important property and can be utilized for many applications. From a single host lattice the tuning of these many colours is an interesting phenomenon. The corresponding values of CIE 1960 and CIE 1976 have also been evaluated. This property of host lattice is a very important and an interesting feature.

CIE Co-ordinates	CIE 1931		CIE 1960		CIE 1976	
Europium Mole %	x	y	u	v	u′	v′
0.0	0.167	0.247	0.119	0.263	0.119	0.395
0.5	0.268	0.322	0.169	0.3054	0.169	0.458
1.0	0.286	0.354	0.171	0.318	0.171	0.477
1.5	0.355	0.350	0.219	0.323	0.219	0.485
2.0	0.451	0.334	0.295	0.328	0.295	0.492
4.0	0.523	0.319	0.362	0.331	0.362	0.496

Table-4: CIE coordinates of the Europium at different mole percentage.

The doping of europium in Sr_2CeO_4 at different mole percent has been tabulated in table-1. As the percentage of europium was increased there is a remarkable shift in the CIE coordinates. The CIE coordinates changed with the change in Europium doping, when it was 0.5mol% the CIE was x = 0.26, y = 0.32, the emission color moved form blue–green for the undoped to white for the 0.5mol% europium it further improved and was near perfect white with x = 0.35 and y = 0.35 (perfect white being x = 0.33, y = 0.33) when the europium concentration was increased to 1.5mol%. We found that the tuning of host lattice can be

achieved with judicious use of dopants. When the doping percentage was further increased to 2.0mol% then we found that the colour coordinates to be x = 0.45, y = 0.33 and for 4.0mol% the coordinates were x = 0.52, y = 0.31 i.e. the colour shifted from white to pink and finally to red colour. The tuning of color from single host lattice is a new phenomenon and if the materials with such tunability would be available then they can open up new dimensions to the ongoing research and development in the field of phosphors. The color coordinates were also calculated for the CIE 1960 and CIE 1976 and are also tabulated in the table-3. Though we have not addressed to the issue of CRI but we feel that with the large range of wavelengths available from blue to green to yellow to red from the same host is of interest and should give very high CRI values since it has been shown that tetrachromatic light sources (blue = 450, cyan = 510, green = 560, red=620) can have a CRI of 95 and are accepted as suitable for most applications **[40].**

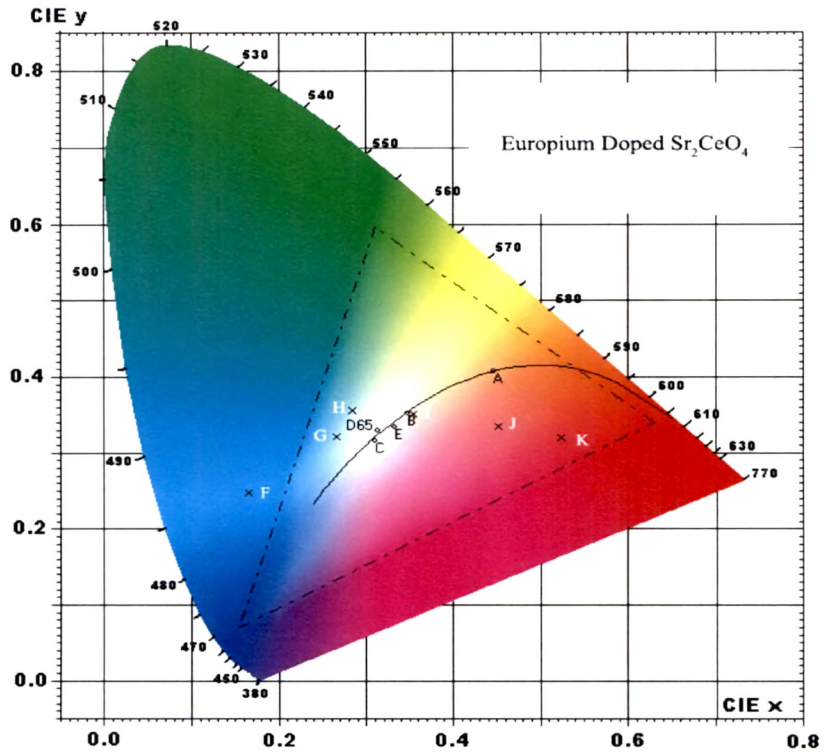

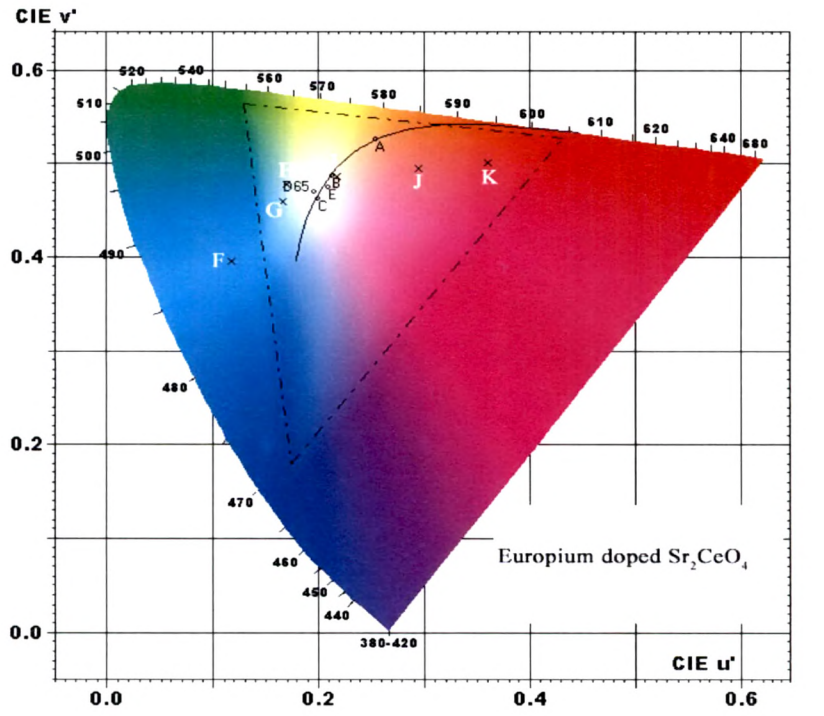

CIE Coordinates depicted on CIE 1931 and CIE 1976 (Where F=0.0, G=0.5, H=1.0, I=1.5, J=2.0, K=4.0mol% of europium doped Sr_2CeO_4).

4.4 Conclusions

The main conclusions that can be drawn by studying the effect of europium doping on the luminescence properties of the Sr_2CeO_4 are as follows:

1. Doping of europium at various concentrations and the study of possible mechanism of energy transfer.
2. Rare europium emission observed at 467nm, the transition being $^5D_2 \rightarrow {}^7F_0$, at room temperature photoluminescence measurements.
3. Comparison with solid state reaction revealed a marked difference in the emission characteristics from 580nm-630nm for the 0.5mol% doped europium sample. This may be due to the formation nanocrystal size (~55nm) of the phosphor with sol-gel technique.
4. Greater splitting of the $^5D_0 \rightarrow {}^7F_1$, $^5D_0 \rightarrow {}^7F_2$ when compared with solid state reaction and few additional lines were seen at 595nm and 611nm for the sol-gel prepared sample.
5. Excellent tunablity of phosphor observed when doped with various concentrations of Europium.
6. The CIE coordinates calculated for all the europium doping concentrations, and they varied from x = 0.26, y = 0.32 to x = 0.52, y = 0.31 i.e. for 0.5mol% and 4.0mol% respectively.
7. White light emission from a single host lattice when the europium concentration was 1.5mol% (x = 0.35, y = 0.35).
8. Nanosize europium doped Sr_2CeO_4 phosphor with high luminescence intensity emission in the white region is achieved due to successful synthesis route i.e. sol-gel.

References

1. G. Blasse and B.C. Grabmaeir, Luminescent Materials, Springer Verlag, Berlin, (**1994**).
2. S. Shionoya, W. Yen, Phosphor Handbook, CRC Press, Boca Raton, (**1999**).
3. Y. Hinatsu, M. Wakeshima, N. Edelstein, I. Craig, Journal of Solid State Chemistry, 144, (**1999**), 20-24.
4. R. Sankar, G.V. Subba Rao, Journal of Electrochemical Society, 147, (**2000**), 2773-2779.
5. A. Nag, T.R.N. Kutty, Journal of Materials Chemistry, 13, (**2003**), 370-376.
6. T. Hirai, Y. Kawamura, Journal of Physical Chemistry B, 108, (**2004**), 12763-12769.
7. T. Hirai, Y. Kawamura, Journal of Physical Chemistry B, 109, (**2005**), 5569-5573.
8. S. Shi, J. Li, J. Zhou, Materials Science Forum, 475-479, (**2005**), 1181-1184.
9. X. Yu, X. Xu, C. Zhou, J. Tang, X. Peng, S. Yang, Materials Research Bulletin, 41, (**2006**), 1578-1583.
10. R. Jagannathan , T.R.N. Kutty, M. Kottaisamy, P. Jeyagopal, Japanese Journal of Applied Physics, 33, (**1994**), 6207-6212.
11. T. Kim, S. Kang, Materials Research Bulletin, 40, (**2005**), 1945-1954.
12. G Concas, G Spano, E Zych, J Trojan-Piegza, Journal of Physics: D Condensed Matter, 17, (**2005**), 2597-2604.
13. K. Lin and Y. Li, Nanotechnology, 17, (**2006**), 4048-4052.
14. J. Dhanaraj, R. Jagannathan, D. C. Trivedi, Journal of Materials Chemistry, 13, (**2003**), 1778-1782.
15. T. Igarashi, M. Ihara, T. Kusunoki, K. Ohno, T. Isobe, M. Senna, Applied Physics Letters, 76, (**2000**), (12).
16. I.L.V. Rosa, A.P. Maciel, E. Longo, E.R. Leite, J.A. Varela, Materials Research Bulletin, 41, (**2006**), 1791-1797.
17. B. Yan, X. Su, K. Zhou, Materials Research Bulletin, 41, (**2006**), 134-143.

18. M. Abdullah, I. W. Lenggoro, B. Xia, K. Okuyama, Journal of the Ceramic Society of Japan, 113, (1), (**2005**), 97-100.

19. G. Wakefield, E. Holland, P. J. Dobson, J.L. Hutchison, Advanced Materials, 13, (**2001**), 20.

20. O. Lehmann, K. Kompe, M. Haase, Journal of American Ceramic Society, 126, (**2004**), 14935-14942.

21. H. Peng, S. Huang, L. Sun, Journal of Luminescence, 122-123, (**2007**), 847-850.

22. Z. Wei, L. Sun, C. Liao, J. Yin, X. Jiang, C. Yan, S. Lu, Journal of Physical Chemistry B, 106, (**2002**), 10610-10617.

23. V. Sudarsan, F.C.J.M. van Veggel, R.A. Herring, M. Raudsepp, Journal of Materials Chemistry, 15, (**2005**), 1332-1342.

24. V. Buissette, D. Giaume, T. Gacoin, J. Boilat, Journal of Materials Chemistry, 16, (2006), 529-539.

25. J. Chang, S. Xiong, H. Peng, L. Sun, S. Lu, F. You, S. Huang, Journal of Luminescence, 122-123, (**2007**), 844-846.

26. A.M. Klonkowski, I. Szalkowska, Materials Science-Poland, 23, 1, (**2005**).

27. M.H.V. Werts, R.T.F. Jukes, W. Verhoeven, Physical Chemistry Chemical Physics, 4, (**2002**), 1542-1548.

28. R. Reisfeld, Materials Science, 20, (2), (**2002**), 5-18.

29. P. Dorenbos, Journal of Luminescence, 111, (**2005**), 89-104.

30. J.R. DiMaio, B. Kokuoz, J. Ballato, Optics Express, 14, (23), (**2006**), 11412-11417.

31. J.S. Kim, P.E. Jeon, J.C. Choi, H.L. Park, S.I. Mho, G.C. Kim, Applied Physics Letters, 84, (**2004**), 2931-2933.

32. T. Jüstel, H. Nikol, C. Ronda, Angewandte Chemie International Edition, 37, (**1998**), 3084-3103.

33. D.A. Steigerwald, J.C. Bhat, D. Collins, R.M. Fletcher, M.O. Holcomb, M.J. Ludowise, P.S. Martin, S.L. Rudaz, IEEE J. Selc Top Quantum Electronics, 8, (**2002**), 310-320.

34. R.P. Rao, Journal of the Electrochemical Society, 150, (8), (**2003**), H165-H171.

35. G. Wakefield, H.A. Keron, P.J. Dobson, J.L. Hutchison, Journal of Colloid and Interface Science, 215, (**1999**), 179-182.

36. R. Ghildiyal, P. Page, K.V.R. Murthy, Journal of Luminescence, 124, (**2007**), 217-220.

37. E. Danielson, M. Devenney, D. Giaquinta, J.H. Golden, R.C. Haushalter, W. McFarland, D.M. Poojary, C.M. Reaves, W.H. Weinberg, X.D. Wu, Science, 279, (**1998**), 837.

38. R.Y. Wang, Journal of Luminescence, 106, (**2004**), 211-217.

39. R.D. Shannon, Acta Crystallographica, A32, (**1976**), 751-767.

40. E.F. Schubert, J.K. Kim, Science, 308, (**2005**), 1274-1278.